

Optimum Noise Mechanism for Differentially Private Queries in Discrete Finite Sets

Sachin Kadam, Anna Scaglione, Nikhil Ravi, Sean Peisert, Brent Lunghino, and Aram Shumavon

Abstract—In this paper, we provide an optimal additive noise mechanism for database queries with discrete answers on a finite support. The noise provides the minimum error rate for a given (ϵ, δ) pair. Popular schemes apply random additive noise with infinite support and then clamp the resulting query response to the desired range. Clamping, unfortunately, compromises the privacy guarantees. Using modulo addition, rather than clamping, we show that, for any (ϵ, δ) pair, the optimum additive noise distribution can be obtained by solving a mixed integer linear program (MILP). Having introduced our optimal noise design formulation, we derive closed form solutions for the optimal noise probability mass function (PMF) and the probability of error for two special cases. In our performance studies, we show that the proposed optimal mechanism outperforms state of the art for a given probability of error and for any budget $\epsilon > 0$.

I. INTRODUCTION

Differential Privacy (DP) is a technique that can be used for publishing database queries without revealing the presence or absence of data with sensitive data attributes. Some real world applications of differential privacy are: the US Census 2020 publication using disclosure avoidance system (DAS) [1], Google’s publication of its historical traffic statistics [2], Microsoft’s publication of telemetry data [3], LinkedIn providing its user engagement information to advertisement companies [4], etc. DP hinges on a randomized mechanism through which the data publisher, who owns the database, responds to the queries of an analyst, so that queries to data that differ by a specific attribute generate a similar distribution of query answers, which in turn makes it statistically hard to reveal whether or not data with that specific attribute were present. Our focus in this paper is in revisiting the design of the private randomized mechanism for discrete queries, for example queries where the answer is an integer number. Our noise mechanism is applicable to any query that has a finite number of answers, where the objective is to meet the DP constraints while minimizing the error rate.

A popular approach in DP is to add zero mean noise to the true answer. In this approach when the query has infinite support, the randomized query response is unbiased. When queries

have a bounded support this is no longer true. Furthermore, the randomized response has a range that overshoots the original query support, causing privacy leakage when the query is at the edge of its possible values. To avoid this situation the typical approach is to clamp randomized answers to be equal to the nearest extreme value in the correct range after adding the noise [5]. Note that, after clamping, the randomized algorithm is no longer independent from the query response, leaking data attributes that lead to such edge values. Another type of projection is to use a symmetric projection like modular addition, which is the focus of the designs proposed in this paper. Prior to outlining our contributions, next we review the relevant literature.

A. Literature review

In literature, several papers studied the additive noise mechanisms for discrete query outputs [6]–[8]. For discrete queries with infinite support, the additive noise mechanism for ϵ -differential privacy that minimizes any convex function of the query error was found in [8]; the optimum PMF is shown to have a specific decreasing staircase trend. The problem of finding the optimal data-independent noise mechanism for ϵ -differential privacy is addressed also in [6]. Even though the authors focus on continuous query outputs, they claim one can extend easily the method to discrete queries. Neither paper [6], [8] explored the optimization of the (ϵ, δ) -differential privacy trade-off for $\delta > 0$. For integer query outputs the optimal noise mechanism design for (ϵ, δ) -differential privacy is the subject of [7]. Another approach to integer count query is carried out in [5], where a double-sided geometric distribution noise mechanism is used. A recent study on the count query DP problem is found in [9], in which the authors use a set of constrained mechanisms that achieve favorable DP properties. The related problem of publishing the number of users with sensitive attributes from a database is addressed in [10]. In their proposed DP mechanism, they add an integer valued noise before publishing it to protect the privacy of individuals. Though the randomized query response, produced by the proposed mechanism in [10], lies in the actual query support range, the additive noise PMF used depends on the query output. In the context of discrete queries, an additive discrete Gaussian noise based mechanism is proposed in [11]. They show that addition of discrete Gaussian noise provides the same privacy and accuracy guarantees as the addition of continuous Gaussian noise.

S. Kadam is with Arizona State University, e-mail: skadam6@asu.edu, A. Scaglione and N. Ravi are with Cornell Tech, e-mail: as337@cornell.edu, nr337@cornell.edu, S. Peisert is with Lawrence Berkeley National Laboratory, e-mail: speisert@lbl.gov, B. Lunghino and A. Shumavon are with Kevala, Inc., e-mail: brent@kevalaanalytics.com, aram@kevalaanalytics.com.

This research was supported by the Director, Cybersecurity, Energy Security, and Emergency Response, Cybersecurity for Energy Delivery Systems program, of the U.S. Department of Energy, under contract DE-AC02-05CH11231. Any opinions, findings, conclusions, or recommendations expressed in this material are those of the authors and do not necessarily reflect those of the sponsors of this work.

B. Paper contributions

This paper revisits the design of a DP random mechanisms to ensure queries answers are (ϵ, δ) differentially private, for queries that can have $n + 1$ possible answers, each mapped onto one of the numbers between $0, \dots, n$. The mechanism we study is the modulo $n + 1$ addition of noise. In Section III-A we show that, for a given (ϵ, δ) budget, the additive noise Probability Mass Function (PMF) that minimizes a linear error metric can be obtained as the solution of a Mixed Integer Linear Program (MILP) in general. Note that, for the case $\delta = 0$ it is already known that the optimum PMF can be found as the solution of an LP problem [12], which is a special case of our general formulation. We then derive the explicit expression of the optimum PMF giving a minimum error for a certain (ϵ, δ) pair for two special cases in Sections III-B1 and III-B2 (which subsumes [12] result). The two cases define specific ways in which data X and X' , that differ because of a sensitive attribute change, can affect the modulo n differences of the query answers. In both cases, we derive the parameters of the error rate function $\rho(\epsilon, \delta)$ showing that it is piece-wise linear. The structure of the optimum PMF and error rate allows us to specify that the optimum (ϵ, δ) trade-off curve for a given error rate is decreasing exponentially as δ increases with a discrete set of discontinuities that prelude a change in the exponential rate of decay as ϵ increases. All of these results are corroborated by our numerical analysis in Section IV with comparisons of the optimum noise mechanism with the prior art.

Notation – Let $\mathbb{N}, \mathbb{Z}, \mathbb{R}$ denote the set of natural numbers, integers, and real numbers, respectively. For positive integers $n, n_1, n_2 \in \mathbb{N} \cup \{0\} \equiv \mathbb{N}^+$, we use $[n]$, $[n]_+$, and $[n_1 : n_2]$ to denote the sets $\{0, 1, \dots, n\}$, $\{1, \dots, n\}$, and $\{n_1, \dots, n_2\}$ respectively. We use boldface letter to denote a vector quantity. $[k]$ denotes the largest integer $\leq k$, i.e., the floor function of k and $\lceil k \rceil$ denotes the smallest integer $\geq k$, i.e., the ceil function of k , respectively. $|\mathcal{A}|$ denotes the cardinality of set \mathcal{A} . Boldface letters are arrays. $\mathbb{Q}(X)$ denotes the query applied on the data X from a database. The entire collection of data in the database is denoted by \mathcal{X} . In this paper, the domain of the query is discrete and finite and is mapped onto the set $[n]$ of size $n+1$. The numerical outcome of the query will be denoted by $q \in [n]$ if it is a scalar and \mathbf{q} for vector queries, while $\tilde{q} \in [n]$ will denote the outcome after the randomized publication. For vector queries \mathbf{q} we consider only the case in which $\mathbf{q} \in [n]^k$. We omit the suffix η from the noise distribution $f_\eta(\eta)$ using the notation $f(\eta)$.

II. PRELIMINARIES

Conventionally, given the random published answer \tilde{q} in the differential privacy literature, the *privacy loss* function name is a synonym for the log-likelihood ratio:

$$L_{xx'}(\tilde{q}) \triangleq \ln \frac{f_{\tilde{q}}(\tilde{q}|X)}{f_{\tilde{q}}(\tilde{q}|X')}, \quad \forall \tilde{q} \in [n]^k, \quad (1)$$

where $X \in \mathcal{X}$ and $X' \in \mathcal{X}_X^{(1)}$, neighbourhood set of X which contains all data sets $X' \in \mathcal{X}$ that differ from X by a predefined sensitive attribute. The reason for the name is

that, in classical statistical inference, $L_{xx'}(\tilde{q}) > 0$ yields the decision that $\tilde{q} \sim f_{\tilde{q}|X}$, where $f_{\tilde{q}|X}$ is the vector containing entries of all the values of $f(\tilde{q}|X)$, for $\tilde{q} \in \mathcal{Q}$ and the symbol \sim refers to the fact that the random variable has that specific distribution. Note that, if the event $L_{xx'}(\tilde{q}) > 0$ is infrequent, then often an alternative hypothesis X' (where the emission probability is $f_{\tilde{q}|X'}$) will be chosen as the correct probabilistic model, which in turn means that the query answer \tilde{q} leaks little information about the attributes that differentiate X from X' . We now review the definition of (ϵ, δ) differential privacy we consider in this paper, which applies to any random vector \tilde{q} for any given X :

Definition 1 ((ϵ, δ) Differential Privacy [13]). *Consider random data that can come from a set of emission probabilities $\tilde{q} \sim f(\tilde{q}|X)$ that change depending on $X \in \mathcal{X}$. The data \tilde{q} are (ϵ, δ) differentially private $\forall X \in \mathcal{X}$ and $X' \in \mathcal{X}_X^{(1)}$, iff:*

$$\delta \geq \delta_q^\epsilon \triangleq \sup_{X \in \mathcal{X}} \sup_{X' \in \mathcal{X}_X^{(1)}} \Pr(L_{xx'}(\tilde{q}) > \epsilon). \quad (2)$$

In our setup $\mathbb{Q}(X)$ is a scalar value in $\mathcal{Q} \equiv [n]$. The query response \tilde{q} is obtained by adding a discrete noise η , whose distribution is denoted by $f(\eta)$, i.e.:

$$\tilde{q} = \mathbb{Q}(X) + \eta \Rightarrow f_{\tilde{q}}(\tilde{q}|X) = f(\tilde{q} - \mathbb{Q}(X)). \quad (3)$$

The PMF associated with the privacy loss function, called privacy leakage probability, for the additive noise mechanism can be derived from (1), (2) and (3):

$$\Pr(L_{xx'}(\tilde{q}) > \epsilon) = \Pr\left(\ln \frac{f(\tilde{q} - \mathbb{Q}(X))}{f(\tilde{q} - \mathbb{Q}(X'))} > \epsilon\right). \quad (4)$$

For the discrete query case, we denote the “distance one set” of $X \in \mathcal{X}$ as $\mathcal{X}_X^{(1)} = \mathcal{X} \setminus X$ and let:

$$\mu_{xx'} \triangleq \mathbb{Q}(X) - \mathbb{Q}(X'), \quad \forall X \in \mathcal{X}, \forall X' \in \mathcal{X}_X^{(1)}. \quad (5)$$

where X' differ from X for one user data record or a sensitive user attribute. Let us define the indicator function $u_{xx'}(\eta)$, $\eta \in [n]$ such that i^{th} entry is one if $L_{xx'}(\tilde{q}_i) > \epsilon$ and zero otherwise, i.e.:

$$u_{xx'}(\eta) \triangleq \begin{cases} 1, & f(\eta) > e^\epsilon f(\eta + \mu_{xx'}) \\ 0, & \text{otherwise.} \end{cases} \quad (6)$$

It is easy to verify that we have:

$$\Pr(L_{xx'}(\tilde{q}) > \epsilon) = \sum_{\eta=0}^n u_{xx'}(\eta) f(\eta).$$

In this paper, we seek to maximize the accuracy or minimize the probability of error, while ensuring a desired (ϵ, δ) DP guarantee. There are two typical metrics:

Definition 2 (Error Rate). *For a discrete query output $\tilde{q} = \mathbb{Q}(X) + \eta$, the error rate is:*

$$\rho^{ER} \triangleq \Pr(\tilde{q} \neq \mathbb{Q}(X)) \quad (7a)$$

$$= 1 - \Pr(\eta = 0) = 1 - f(0). \quad (7b)$$

This metric makes sense when it does not matter what value the query response \tilde{q} has taken that is not equal to the

true value $\mathbb{Q}(X)$. Another possible measure of error is mean squared error (MSE), specified as follows:

Definition 3 (Mean Squared Error). For a discrete query output $\tilde{q} = \mathbb{Q}(X) + \eta$, the mean squared error (MSE) is:

$$\rho^{MSE} \triangleq \mathbb{E}[|\tilde{q} - \mathbb{Q}(X)|^2] = \sum_{\eta=1}^n \eta^2 f(\eta). \quad (8)$$

Because our analytical results consider the error rate metric, whenever ρ is mentioned without specification, this implies ρ^{ER} is being discussed.

III. OPTIMAL ADDITIVE NOISE

In this paper we seek to obtain the optimum noise mechanism using modular addition of noise to the discrete query. For queries $q = \mathbb{Q}(X) \in [n]$, a possible approach other than clamping is to assume that the noise addition is modulo $n+1$ with $\eta \in [n]$, so that the outcome $\tilde{q} = q + \eta \pmod{n+1}$, is always in the appropriate range. We omit the $\pmod{n+1}$ to streamline the notation, with the understanding that, from now on, sums and differences of query outcomes and of noise values are always modulo $n+1$. A first observation is that adding uniform noise would lead necessarily to a scalar query \tilde{q} being uniform and thus, high privacy (i.e. $\delta = 0$ for any $\epsilon > 0$) but poor accuracy since $\rho^{ER} = 1 - 1/(n+1)$. A second observation is that only the uniform distribution will give an unbiased answer. Using (4) and (5):

$$Pr(L_{xx'}(\tilde{q}) > \epsilon) = Pr\left(\ln \frac{f(\tilde{q} - \mathbb{Q}(X))}{f(\tilde{q} - \mathbb{Q}(X'))} > \epsilon\right) \quad (9a)$$

$$= Pr\left(\ln \frac{f(\eta)}{f(\eta + \mu_{xx'})} > \epsilon\right). \quad (9b)$$

From (9b) it is evident that the (ϵ, δ) privacy curve is entirely defined by the noise distribution and its change due to a shift in the mean. As a result, the probability mass $f(q + \eta)$ is obtained as a circular shift of the PMF $f(\eta)$; therefore (9b) can be used with the denominator $f(\eta + \mu_{xx'})$ also representing a circular shift of $f(\eta)$.

From (9b) it is apparent that the interplay of noise distribution and the possible values for the offset $\mu_{xx'}$ are all that are needed to establish the (ϵ, δ) privacy trade-off. This result motivates us to define the neighbourhood sets, using only $\mu_{xx'}$, in the following subsection.

A. Numerical Optimization

In this section, we show that the problem of finding an optimal additive noise mechanism for a given pair (ϵ, δ) can be cast into a Mixed Integer Linear Program (MILP) formulation. Though the formulation can be generalized to find an optimum design that minimizes any expected cost, we focus on the error rate cost case (see Definition 2) to find closed form solutions. We can rewrite (9b) as $Pr(L_{xx'}(\tilde{q}) > \epsilon) = Pr(f(\eta) > e^\epsilon f(\eta + \mu_{xx'}))$. From Definition 1 and (6), we can write δ , which is a privacy loss bound, in terms of a constraint: $\sum_{\eta=0}^n u_{xx'}(\eta) f(\eta) \leq \delta, \forall X \in \mathcal{X}, \forall X' \in \mathcal{X}_X^{(1)}$. Since it is a

bilinear constraint, we define auxiliary variables $y_\eta, \eta \in [n]$ as follows:

$$y_\eta \triangleq u_{xx'}(\eta) f(\eta), \quad \eta \in [n]. \quad (10)$$

We can add the two constraints $u_{xx'}(\eta) + f(\eta) - y_\eta \leq 1$, $u_{xx'}(\eta) - f(\eta) + y_\eta \leq 1$,¹ and $y_\eta - u_{xx'}(\eta) \leq 0$ ² to make non linear constraints linear. The MILP formulation is:

$$\min_{f_\eta, \forall X \in \mathcal{X}, \forall X' \in \mathcal{X}_X^{(1)}} \sum_{\eta=1}^n f(\eta) \quad (11a)$$

$$\sum_{\eta=0}^n f(\eta) = 1, \quad \sum_{\eta=1}^n f(\eta) < 0.5, \quad (11b)$$

$$\sum_{\eta=0}^n y_\eta \leq \delta, \quad y_\eta - u_{xx'}(\eta) \leq 0, \quad (11c)$$

$$u_{xx'}(\eta) + f(\eta) - y_\eta \leq 1, \quad (11d)$$

$$u_{xx'}(\eta) - f(\eta) + y_\eta \leq 1, \quad (11e)$$

$$f(\eta) - e^\epsilon f(\eta + \mu_{xx'}) - u_{xx'}(\eta) \leq 0, \quad (11f)$$

$$e^\epsilon f(\eta + \mu_{xx'}) - f(\eta) + e^\epsilon u_{xx'}(\eta) \leq e^\epsilon, \quad (11f)$$

$$f(\eta), y_\eta \in [0, 1] \quad \eta \in [n], \quad u_{xx'}(\eta) \in \{0, 1\}.$$

The MILP has $3(n+1)$ variables out of which the $n+1$ $f(\eta)$ and y_η are real numbers in $[0, 1]$ and $u_{xx'}(\eta)$ (which are also $(n+1)$) are binary; $(3n+5) + 2(n+1)|\{\mu_{xx'}\}|$ inequality constraints and 1 equality constraint. For $\delta = 0$ the MILP reduces to the linear program (LP):

$$\min_{f_\eta, \forall X \in \mathcal{X}, \forall X' \in \mathcal{X}_X^{(1)}} \sum_{\eta=1}^n f(\eta) \quad (12a)$$

$$\sum_{\eta=0}^n f(\eta) = 1, \quad \sum_{\eta=1}^n f(\eta) < 0.5, \quad (12b)$$

$$f(\eta) - e^\epsilon f(\eta + \mu_{xx'}) \leq 0, \quad \eta \in [n], \quad (12c)$$

$$f(\eta) \in [0, 1]. \quad (12d)$$

Remark 1. It is worth noting that the MILP formulation can be extended straightforwardly to different expected costs definitions, by replacing the objective with a weighted linear combination of $f(\eta)$, $\rho = \sum_{\eta=1}^n w_\eta f(\eta)$, as well as to the minimization of δ , which is the term $\sum_{\eta=0}^n y_\eta \leq \delta$, in (11c), for a given ϵ and accuracy constraint. In the latter case the accuracy cost, i.e., error rate ρ , can be placed as a constraint.

Note that since we are finding the optimum noise mechanism based on modulo addition between the query and the noise, we use modulo $(n+1)$ sum of η and $\mu_{xx'}$ in (11e), (11f), and (12c).³ This modulo operation makes these constraints circular. In the next sections we derive analytical solutions for some special database structures and corroborate the results in Section IV comparing the formulas with the MILP solutions obtained using Gurobi [14] as a solver.

¹These two inequalities make sure that $y_\eta = f(\eta)$, whenever $u_{xx'}(\eta) = 1$.

²This inequality makes sure that $y_\eta = 0$, whenever $u_{xx'}(\eta) = 0$.

³This notation convention is mentioned at the beginning of Section III.

B. Analytical Solutions

To give closed-form solutions for the optimum PMF, we focus on the following instances of possible $\mu_{xx'}$:

Definition 4 (Single Distance). In this setting $\forall X \in \mathcal{X}, \forall X' \in \mathcal{X}_X^{(1)}$, the difference $\mu_{xx'}$ is constant, i.e. $\mu_{xx'} = \hat{\mu}$. Note that $\hat{\mu} \leq n$.

Definition 5 (Bounded Difference). In this setting $\forall X \in \mathcal{X}, \forall X' \in \mathcal{X}_X^{(1)}$ $\mu_{xx'}$ take values in the set $[\bar{\mu}]_+$, $\bar{\mu} \leq n$, at least once.

The most general case is the following:

Definition 6 (Arbitrary). In this case $\mu_{xx'}$ can take values from any subset of $[n]$, $\forall X \in \mathcal{X}, \forall X' \in \mathcal{X}_X^{(1)}$.

The next lemma clarifies that the optimum PMF for the BD case for a given (ϵ, δ) is useful to attain the same guarantees for the case of arbitrary neighborhood.

Lemma 1. Suppose $\bar{\mu} = \sup_{\forall X \in \mathcal{X}, \forall X' \in \mathcal{X}_X^{(1)}} \mu_{xx'}$. Then any noise PMF that provides (ϵ, δ) privacy for the bounded difference (BD) neighborhood with parameter $\bar{\mu}$ will give the same guarantees in terms of (ϵ, δ) and ρ for the case of arbitrary neighborhoods. However, lower distortion is achievable solving the MILP.

Proof. The proof is simple: the set of constraints that need to be met to satisfy (ϵ, δ) privacy for the arbitrary case is a subset of the BD neighborhood case with $\bar{\mu}$ as a parameter. This also means, however, that the minimum ρ^* for the latter case is sub-optimum. \square

Note that single distance (SD) neighbourhood setting is a simple case while the previous lemma indicates that the BD case is more useful in general. It is easy to analyse and helpful in developing theories and designing mechanisms. It can be used as a building block for designing mechanisms for a practically possible bounded difference neighbourhood setting. We also provide the numerical results of our optimization for an arbitrary neighbourhood setting in Section IV.

Next we find an explicit solution for the optimum noise PMF $f^*(\eta), \eta \in [n]$ for the SD and BD neighbourhood cases, in Definition 4 and 5 respectively. In Section III-B4, we discuss the case of discrete vector queries.

1) *PMF for Single Distance Neighbourhood:* The natural way to express the optimum PMF for an SD neighbourhood setting is by specifying the probability masses in a sorted decreasing ordered set of $f(k), \forall k \in [n]$, for which we use the notation $\{f(k) | 1 \geq f(0) \geq f(1) \geq \dots \geq f(n) \geq 0\}$.

Lemma 2. Considering the case in Definition 4 where $\mu_{xx'} = \hat{\mu}$ is constant $\forall X \in \mathcal{X}, \forall X' \in \mathcal{X}_X^{(1)}$, the noise PMF minimizing the error rate is such that $f_{(h)}^* = f^*(h\hat{\mu}), \forall h \in [n]$ and the inequality in (12c), can be written in term of the sorted PMF as follows:

$$f_{(h)}^* - e^\epsilon f_{(h+1)}^* \leq 0, \quad \forall h \in [n]. \quad (13)$$

Proof. The proof is in Appendix A. \square

To start, let us consider the case $\delta = 0$; it holds:

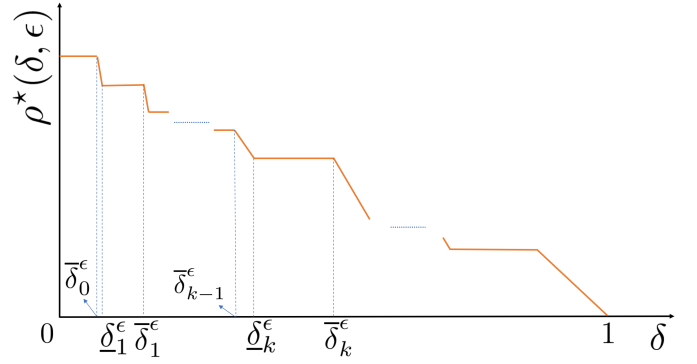


Fig. 1: The variation of ρ as a function of δ for single distance (SD) neighbourhood showing the alternate flat and linear regions.

Lemma 3. For the SD neighborhood and $\delta = 0$ the optimal noise PMF for the modulo addition mechanism is:

Case 1: If $(\hat{\mu}, (n+1))$ are relatively prime.

$$f_{(k)}^* = e^{-k\epsilon} f_{(0)}^*, \quad k \in [n]_+, \quad (14a)$$

$$f_{(0)}^* = \frac{1 - e^{-\epsilon}}{1 - e^{-(n+1)\epsilon}} \equiv f^*(0). \quad (14b)$$

Case 2: If $(\hat{\mu}, (n+1))$ are not relatively prime:

$$f_{(k)}^* = e^{-k\epsilon} f_{(0)}^*, \quad k \in [N_{\hat{\mu}} - 1]_+ \quad (15a)$$

$$f_{(k)}^* = 0, \quad k \in [n] \setminus [i\hat{\mu}], \quad \forall i \in [N_{\hat{\mu}} - 1] \quad (15b)$$

$$f_{(0)}^* = \frac{1 - e^{-\epsilon}}{1 - e^{-N_{\hat{\mu}}\epsilon}} \equiv f^*(0). \quad (15c)$$

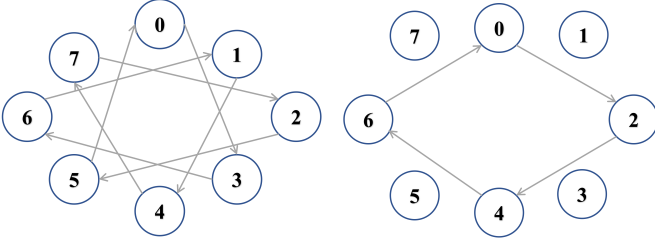
where $N_{\hat{\mu}} = \frac{(n+1)}{\gcd((n+1), \hat{\mu})}$ and $\rho^* = 1 - f^*(0)$.

Proof. The proof is in Appendix B. \square

Lemma 3 is verified numerically in Section IV in both Case 1 and 2 (see Fig. 7). We illustrate the two cases in Fig. 2. From (14b) we can observe that for case 1, the error rate ρ^* depends only on ϵ and n , and for case 2 (see (15c)), ρ^* depends on both ϵ and $N_{\hat{\mu}}$.

Mechanisms with better error rate (lower ρ) must allow for $\delta > 0$. It can be proven (see Theorem 1) that the optimal error rate $\rho^*(\delta, \epsilon)$ vs. δ curve is piece-wise linear, interleaving flat regions with intervals with linear negative slope, see Fig. 1. We categorize them as “linear region” and “flat region”. Let δ_k^ϵ and $\bar{\delta}_k^\epsilon$ be the instances of δ at which $\rho^*(\delta, \epsilon)$ changes from k^{th} linear region to k^{th} flat region and k^{th} flat region to $(k+1)^{th}$ linear region, respectively.

Remark 2. We state the following results of this section, i.e., Section III-B1, for the case $(n+1, \hat{\mu})$ that are relatively prime. For the case in which they are not, the results are obtained by replacing n with $N_{\hat{\mu}} = \frac{(n+1)}{\gcd((n+1), \hat{\mu})}$ in all the expressions and explanations.



(a) Case 1: $\hat{\mu} = 3$, $n = 7$, here (3, 8) are relatively prime. (b) Case 2: $\hat{\mu} = 2$, $n = 7$, here (2, 8) are not relatively prime.

Fig. 2: In these examples $f^*(\hat{\mu})$ is single distance, $\hat{\mu}$, away from $f^*(0)$ hence it is assigned $e^{-\epsilon} f^*(0)$, next $f^*(2\hat{\mu})$ is assigned $e^{-2\epsilon} f^*(0)$ since it is $2\hat{\mu}$ away from $f^*(0)$ and so on. So the order of assignment of values for plot (a) example is: 0, 3, 6, 1, 4, 7, 2, 5 and the order of assignment of values for plot (b) example is: 0, 2, 4, 6. Since the values at 1, 3, 5, 7 are not $\hat{\mu}$ away from $f^*(2k\hat{\mu})$, $k \in [N_{\hat{\mu}} - 1] = 3$ they are assigned 0 value to have a higher $f^*(0)$.

Let us define the following quantities:

$$\bar{\delta}_k^\epsilon := e^{-(n-k-1)\epsilon} \frac{1 - e^{-\epsilon}}{1 - e^{-(n-k+1)\epsilon}}, \text{ for } k \in [n-1] \quad (16a)$$

$$\bar{\delta}_n^\epsilon := 1 \quad (16b)$$

$$\underline{\delta}_0^\epsilon := 0 \quad (16c)$$

$$\underline{\delta}_k^\epsilon := e^{-(n-k)\epsilon} \frac{1 - e^{-\epsilon}}{1 - e^{-(n-k+1)\epsilon}}, \text{ for } k \in [n]_+. \quad (16d)$$

Theorem 1. For a given $\epsilon > 0$, the minimum error rate $\rho^*(\delta, \epsilon)$ for $\mu_{xx'} = \hat{\mu}$, $\forall X \in \mathcal{X}, \forall X' \in \mathcal{X}_X^{(1)}$ (i.e. the SD neighbourhood) is a piece-wise linear function with respect to $\delta \in [0, 1]$ and the entries of optimum PMF sorted in decreasing order, similarly, alternates k different trends depending on the values of δ . Specifically, for $k = 0$, the expressions of $f_{(h)}^*$ in Lemma 3 are valid between $0 = \underline{\delta}_0^\epsilon \leq \delta \leq \bar{\delta}_0^\epsilon$. For the remaining $k \in [n]_+$, in the k^{th} section where $\rho^*(\delta, \epsilon)$ is flat within $\underline{\delta}_k^\epsilon \leq \delta \leq \bar{\delta}_k^\epsilon$:

$$f_{(h)}^* = \begin{cases} \bar{\delta}_k^\epsilon e^{(n-k-h)\epsilon}, & h \in [n-k], \\ 0, & h \in [n-k+1 : n], \end{cases} \quad (17)$$

In the portion of the k^{th} section where $\rho^*(\delta, \epsilon)$ decreases linearly with δ , which are within $\bar{\delta}_{k-1}^\epsilon < \delta \leq \bar{\delta}_k^\epsilon$:

$$f_{(h)}^* = \begin{cases} \delta e^{(n-k-h)\epsilon}, & h \in [n-k], \\ e^{(n-h)\epsilon} \frac{e^{-\epsilon} - 1}{e^{k\epsilon} - 1} \left(1 - \frac{\delta}{\bar{\delta}_k^\epsilon}\right), & h \in [n-k+1 : n]. \end{cases} \quad (18)$$

and $\rho^*(\delta, \epsilon) = 1 - f_{(0)}^*$.

Proof. The proof is in Appendix C. \square

From Theorem 1 we note that the boundary point $\underline{\delta}_k^\epsilon$ indicates the value of $f_{(n-k)}^*$, which is the smallest non-zero probability mass in the k^{th} flat region. Similarly, the other boundary point $\bar{\delta}_k^\epsilon \equiv e^\epsilon \underline{\delta}_k^\epsilon$ indicates the value of $f_{(n-k-1)}^*$, which is the smallest non-zero probability mass in the $(k-1)^{\text{th}}$ flat region. Having calculated the optimal PMF for the SD neighbourhood case in Theorem 1, the (ϵ, δ) curves correspond to $f^*(0) = 1 - \rho^*$ for all its $n+1$ possible expressions or,

better stated, they are the level curves $\rho(\delta, \epsilon) = \rho^*$. The trend of δ curves is monotonically decreasing with respect to ϵ for a given ρ^* . Let $\epsilon_0^{\rho^*}$ be the solution obtained setting $f^*(0)$ in (14b) to be equal to $1 - \rho^*$, i.e.:

$$\epsilon_0^{\rho^*} : \rho^* = 1 - \frac{1 - e^{-\epsilon_0^{\rho^*}}}{1 - e^{-(n+1)\epsilon_0^{\rho^*}}} \quad (19)$$

Then we must have that $\delta = 0$ at $\epsilon \geq \epsilon_0^{\rho^*}$. Because this corresponds to a flat region for $f^*(0)$, there has to be a discontinuity moving towards lower values $\epsilon < \epsilon_0^{\rho^*}$, and δ must immediately jump to $\bar{\delta}_0^{\rho^*}$ as soon as one moves to an infinitesimal amount below $\epsilon_0^{\rho^*}$. This point is the edge of the linear region. For a range of values of $\epsilon < \epsilon_0^{\rho^*}$, δ with respect to ϵ must have the negative exponential trend $\delta = (1 - \rho^*)e^{-n\epsilon}$ obtained from equation (18) for $h = 0, k = 1$ until the next jump occurs, for a value $\epsilon_1^{\rho^*}$ which is obtained by setting $f^*(0)$ for $h = 0$ and $k = 1$ in (17) to be equal to $1 - \rho^*$:

$$\epsilon_1^{\rho^*} : \rho^* = 1 - \bar{\delta}_1^{\epsilon_1^{\rho^*}} e^{(n-1)\epsilon_1^{\rho^*}} = 1 - \frac{1 - e^{-\epsilon_1^{\rho^*}}}{1 - e^{-n\epsilon_1^{\rho^*}}}. \quad (20)$$

Following this logic, one can prove that the optimum (ϵ, δ) curve for a given error rate ρ^* is:

Corollary 1. For a given $\epsilon > 0$, the privacy loss for the SD neighbourhood case with the optimal noise mechanism, is a discontinuous function of ϵ , where:

$$\delta^\epsilon = e^{-(n-k)\epsilon} (1 - \rho^*), \quad \epsilon_k^{\rho^*} \leq \epsilon < \epsilon_{k-1}^{\rho^*} \quad (21)$$

when $\rho^* = 1 - f_{(0)}^*$ is in k^{th} section, $k \in [n]_+$ and $\epsilon_k^{\rho^*}$ are the solutions of the following equations:

$$\epsilon_k^{\rho^*} : \rho^* = 1 - \bar{\delta}_k^{\epsilon_k^{\rho^*}} e^{(n-k)\epsilon_k^{\rho^*}} = 1 - \frac{1 - e^{-\epsilon_k^{\rho^*}}}{1 - e^{-(n+1-k)\epsilon_k^{\rho^*}}}. \quad (22)$$

Proof. As discussed before the Corollary the level curves of $\rho^*(\delta, \epsilon) = \rho^*$ as a function of ϵ must be monotonically decreasing as ϵ increases, with $\delta = 0$ for $\epsilon \geq \epsilon_0^{\rho^*}$ in (19). Then the curve will have discontinuities that correspond to the flat regions and the trend between these discontinuities is obtained through the equation $(1 - \rho^*) = f^*(0) = \delta e^{(n-k)\epsilon}$, which implies $\delta = (1 - \rho^*)e^{-(n-k)\epsilon}$. The k^{th} interval starts at the point $\epsilon = \epsilon_k^{\rho^*}$ such that $\delta = \underline{\delta}_k^{\epsilon_k^{\rho^*}}$ ensures that $f^*(0) = 1 - \rho^*$; thus, $\epsilon = \epsilon_k^{\rho^*}$ must be the solution of (22). \square

2) *The Bounded Difference (BD) Neighbourhood:* Also in this case we first start with the optimum noise for $\delta = 0$. First, let us express n as:

$$n = b\bar{\mu} + r \quad (23)$$

where $b = \lfloor n/\bar{\mu} \rfloor$ and $r \in [\bar{\mu} - 1]$. For this case, the inequalities in (12c) can be written as the following:

$$f^*(h) - e^\epsilon f^*(h + \mu) \leq 0, \quad \forall h \in [n], \forall \mu \in [\bar{\mu}]_+. \quad (24)$$

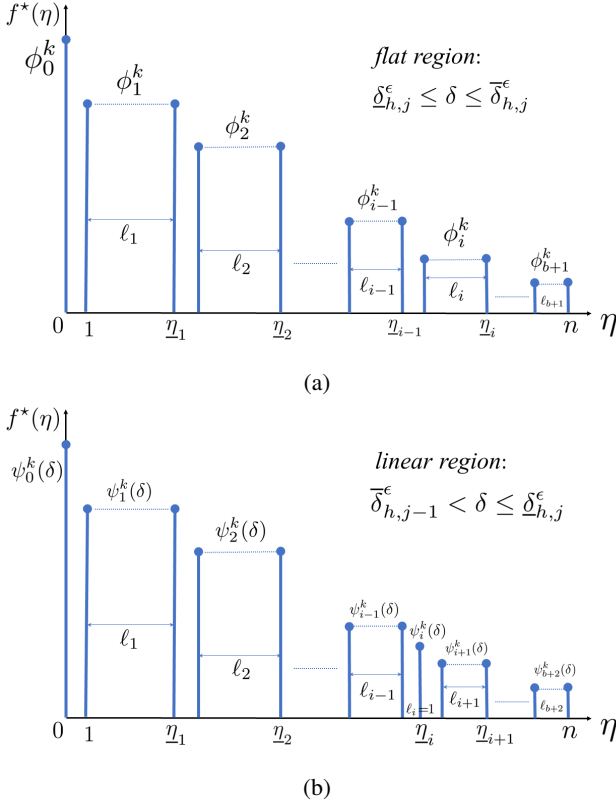


Fig. 3: The PMF of the optimal noise mechanism for BD neighbourhood follows a staircase pattern. In the flat region, it has $b + 1$ steps and i^{th} step height is ϕ_i^k . Similarly, in the linear region, the PMF has $b + 2$ steps and i^{th} step height is $\psi_i^k(\delta)$.

Lemma 4. If $\forall X \in \mathcal{X}, \forall X' \in \mathcal{X}_X^{(1)}$ the sets have $\mu_{xx'}$ which lie in a BD neighbourhood of size $\bar{\mu}$, the optimum PMF $f^*(\eta)$ has the following form for $i \in [b+1]_+$:

$$f^*(\eta) = f^*(0)e^{-i\epsilon} \equiv \phi_i, \quad (i-1)\bar{\mu}+1 \leq \eta \leq \min(i\bar{\mu}, n). \quad (25)$$

and the mass at zero is:

$$f^*(0) = \left(1 + \bar{\mu} \sum_{i=1}^b e^{-i\epsilon} + r e^{-(b+1)\epsilon} \right)^{-1} \equiv \phi_0. \quad (26)$$

The PMF has, therefore, a staircase trend with steps of length $\ell_i = \bar{\mu}$ for $i \in [b]_+$ and $\ell_{b+1} = r$ and $\rho^* = 1 - \phi_0$.

Proof. The proof is similar to that of Lemma 3 because it recognizes that it is best to meet the inequalities in (24) as equalities, since that allows for the largest $f^*(0)$. The only difference is that the masses in the first group $[\bar{\mu}]_+$ are equal to $\phi_1 = e^{-\epsilon} f^*(0)$, thus they constrain a second group to have value $\phi_2 = e^{-\epsilon} \phi_1$ and so on. There are b of them that contain $\bar{\mu}$ masses of probability and only the last group includes the last r values. $f^*(0)$ is obtained normalizing the PMF to add up to 1. \square

The PMF for $\delta > 0$ has staircase pattern (see Fig. 3), similar to Lemma 4 and, also in this case, for $\delta > 0$ the $\rho^*(\delta, \epsilon)$ has a piece-wise linear trend that alternates flat and linear regions. However, the BD neighborhood case has an intricate pattern in which the constraints become violations, as the privacy loss

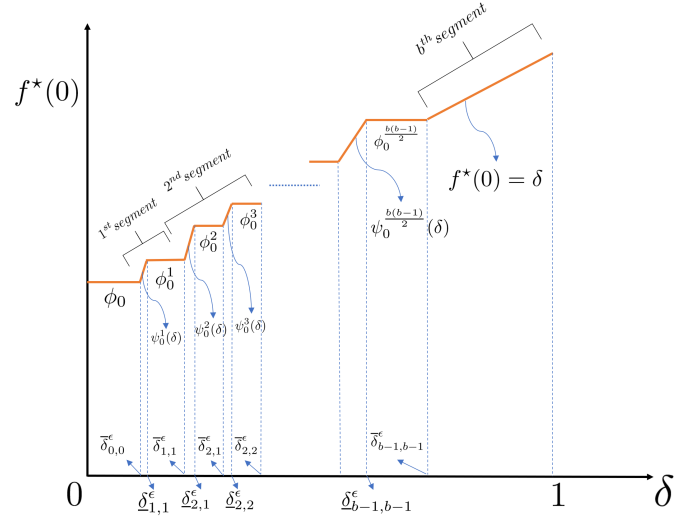


Fig. 4: The variation of $f^*(0)$ as a function of δ for bounded difference (BD) neighbourhood showing b segments with the alternate flat and linear regions.

$\delta \rightarrow 1$. The number of sections k which is quadratic in b rather than having only n of them. To explain the trend, it is best to divide the section of the $f^*(0) \equiv 1 - \rho^*(\delta, \epsilon)$ curve vs. δ in b segments, indexed by $h \in [b]_+$ as shown in Fig. 4. Except for the last interval corresponding to $h = b$, the other segments, indexed by $h \in [b-1]_+$, are further divided into h segments, indexed by $j \in [h]_+$ and this index refers to one of the alternating flat and linear regions within the h^{th} interval. This results in $k = \frac{b(b-1)}{2}$ alternating flat and linear regions. Instead, the segment indexed by $h = b$, there is only one linear region i.e., $f^*(0) = \delta$. The optimum distribution is specified in the following theorem:

Theorem 2. Let $b + r < \bar{\mu}$. For a given $\epsilon > 0$ and for $\mu_{xx'} \in [\bar{\mu}]_+$, $\forall X \in \mathcal{X}, \forall X' \in \mathcal{X}_X^{(1)}$ (i.e. the BD neighbourhood), $f^*(0)$ versus δ features flat and linear regions as shown in Fig. 4. In the first $(b-1)$ segments, indexed by $h \in [b-1]_+$, each alternating a pair of flat and linear regions indexed $j \in [h]_+$, with respective boundaries $\delta_{h,j}^epsilon \leq \delta \leq \delta_{h,j}^epsilon$ and $\delta_{h,j-1}^epsilon < \delta \leq \delta_{h,j}^epsilon$, with the convention $\delta_{h,0}^epsilon = \delta_{h-1,h-1}^epsilon$. The following facts are true:

(a) In the k^{th} flat region, $k = \sum_{j'=1}^{h-1} j' + j = \frac{(h-1)h}{2} + j$, the optimum PMF (c.f. Fig. 3a) for $i \in [b+1]_+$ is:

$$f^*(\eta) = f^*(0)e^{-i\epsilon} \equiv \phi_i^k, \quad \eta_{i-1} < \eta \leq \eta_i, \quad \eta_0 = 0, \quad (27)$$

where what distinguishes the distributions for each k are the intervals $\eta_{i-1} < \eta \leq \eta_i, i \in [b+1]_+$ with equal probability mass ϕ_i^k . More specifically, considering the k^{th} flat region, corresponding to the pair h, j with $h \in [b-1]_+, j \in [h]_+$, the intervals $\eta_{i-1} < \eta \leq \eta_i$ of the optimum PMF have lengths

for $i \in [b+1]_+$:

$$\ell_i = \begin{cases} 1, & \text{for } i = 0 \\ \bar{\mu}, & \text{for } i \in [b-h]_+ \\ \bar{\mu} - 1, & \text{for } i \in [b-h+1:b], i \neq b-h+j+1 \\ \bar{\mu}, & \text{for } i = b-h+j+1 \text{ when } j \neq h \\ r+h-u_{hj}, & \text{for } i = b+1. \end{cases} \quad (28)$$

$$u_{hj} = \begin{cases} 1, & \text{for } j \neq h, \\ 0, & \text{for } j = h. \end{cases} \quad (29)$$

The corresponding indexes sets are obtained as:

$$\eta_0 = 0, \quad \eta_i = \eta_{i-1} + \ell_i, \quad i \in [b+1]_+. \quad (30)$$

To normalize the distribution $f^*(0) = \phi_0^k$ must be:

$$\phi_0^k = \frac{1}{\sum_{i=0}^{b+1} \ell_i e^{-i\epsilon}} = (\bar{\mu}\alpha_{hj}^\epsilon + \beta_{hj}^\epsilon)^{-1}, \quad (31)$$

$$\alpha_{hj}^\epsilon := e^{-\epsilon} \xi_b^\epsilon - (1-u_{hj})e^{-(b-h+j+1)\epsilon}, \quad \xi_a^\epsilon := \sum_{i'=0}^{a-1} e^{-i'\epsilon}, \quad \forall a \in \mathbb{N}^+ \quad (32)$$

$$\beta_{hj}^\epsilon := 1 + e^{-(b-h+1)\epsilon} (e^{-j\epsilon} - \xi_h^\epsilon) + (r+h-u_{hj})e^{-(b+1)\epsilon} \quad (33)$$

and the PMF is valid within $\underline{\delta}_{h,j}^\epsilon \leq \delta \leq \bar{\delta}_{h,j}^\epsilon$ where:

$$\bar{\delta}_{h,j}^\epsilon = \phi_0^k e^{-(b-h)\epsilon} \sum_{j'=0}^j e^{-j'\epsilon} = \phi_0^k e^{-(b-h)\epsilon} \xi_{j+1}^\epsilon, \quad j \in [h-1] \quad (34a)$$

$$\bar{\delta}_{h,h}^\epsilon = \phi_0^k e^{-(b-h-1)\epsilon}, \quad \bar{\delta}_{0,0}^\epsilon = \phi_0 e^{-(b-1)\epsilon}, \quad (34b)$$

$$\underline{\delta}_{h,j}^\epsilon = \phi_0^k e^{-(b-h)\epsilon} \xi_j^\epsilon \equiv \left(\frac{\phi_0^k}{\phi_{0,j}^{k-1}} \right) \bar{\delta}_{h,j-1}^\epsilon \quad (34b)$$

(b) In each of the linear regions, i.e., $\bar{\delta}_{h,j-1}^\epsilon < \delta \leq \underline{\delta}_{h,j}^\epsilon$, the PMF values vary linearly in groups with respect to δ . The group lengths are:

$$\ell_i = \begin{cases} 1, & \text{for } i = 0 \\ \bar{\mu}, & \text{for } i \in [b-h]_+ \\ \bar{\mu} - 1, & \text{for } i \in [b-h+1:b], i \neq b-h+j+1 \\ 1, & \text{for } i = b-h+j+1 \\ r+h-1 & \text{for } i = b+2 \end{cases} \quad (35)$$

each with probability $\psi_i^k(\delta)$ (as shown in Fig. 3b):

$$\psi_i^k(\delta) = \begin{cases} \delta e^{(b-h-i)\epsilon} / \xi_j^\epsilon, & i \in [b-h+j] \\ \delta e^{(b-h-i+1)\epsilon} / \xi_j^\epsilon, & i \in [b-h+j+2:b+2], \end{cases} \quad (36)$$

$$\psi_i^{b-h+j+1}(\delta) = 1 - \sum_{\substack{i=0 \\ i \neq b-h+j+1}}^{b+2} \ell_i \psi_i^k(\delta).$$

(c) In the b^{th} segment, i.e., $\bar{\delta}_{b-1,b-1}^\epsilon < \delta \leq 1$, the objective function, maximize $f^*(0)$, equals to the constraint δ . So any set of $f^*(\eta)$, $\eta \in [n]$, that satisfy $\sum_{\eta=1}^n f^*(\eta) = 1 - \delta$ and

$u_{xx}(0) = 1, u_{xx}(\eta) = 0, \eta \in [n]_+$, provide the optimal PMF. One of the possible solution is:

$$f^*(0) = \delta, \quad (37)$$

$$f^*(\eta) = \frac{1-\delta}{n}, \quad \eta \in [n]_+. \quad (38)$$

Note that in the last segment, optimal PMF do not follow staircase pattern.

Proof. The proof is in Appendix D. \square

Note that, in Theorem 2 we discuss about the case $b+r < \bar{\mu}$. Though the case $b+r \geq \bar{\mu}$ are not conceptually difficult, the optimal PMF is hard to express in a readable form. We discuss the general case towards the end of Appendix D.

Corollary 2. For a given $\epsilon > 0$, the privacy loss for the BD neighbourhood case with the optimal noise mechanism is also a discontinuous function of ϵ , where:

$$\delta^\epsilon = \xi_j^\epsilon e^{-(b-h)\epsilon} (1 - \rho^*), \quad \epsilon_{h,j}^{\rho^*} \leq \epsilon < \epsilon_{h,j-1}^{\rho^*} \quad (39)$$

when $\rho^* = 1 - \psi_0^k(\delta)$ is in k^{th} section, $k \in \left[\frac{b(b-1)}{2} \right]_+$ and $\epsilon_{h,j}^{\rho^*}$, $h \in [b-1]_+$, $j \in [h]_+$, are the solutions of:

$$\epsilon_{h,j}^{\rho^*} : \quad \rho^* = 1 - \phi_0^k = 1 - \left(\bar{\mu}\alpha_b^{\epsilon_{h,j}^{\rho^*}} + \beta_{h,j}^{\epsilon_{h,j}^{\rho^*}} \right)^{-1}. \quad (40)$$

Proof. The proof is a direct extension of that for Corollary 1 and is omitted for brevity. \square

3) *Optimal Error Rates as $n \rightarrow \infty$:* In this section we study the limit for $n \rightarrow \infty$ of the distributions for the two cases we studied, the SD and BD neighborhoods. First, we discuss the $\delta = 0$ case. The goal is to find the relationship between ϵ and ρ when $n \rightarrow \infty$. From Lemma 3 (14b), we see that for SD neighbourhood case, $f^*(0) \equiv 1 - \rho^*(\epsilon) \rightarrow 1 - e^{-\epsilon} \implies \rho^*(\epsilon) \rightarrow e^{-\epsilon}$ as $n \rightarrow \infty$. Since, $\rho^*(\epsilon)$ is also constrained by 0.5, we have that the limit function $\rho_\infty^*(\epsilon)$:

$$\rho_\infty^*(\epsilon) = \begin{cases} 0.5, & \epsilon \in (0, \ln 2] \\ e^{-\epsilon}, & \epsilon \geq \ln 2. \end{cases} \quad (41)$$

And the optimum PMF is zero for all $\eta \neq h\hat{\mu}$, and:

$$f_\infty^*(h\hat{\mu}) = (1 - \rho_\infty^*(\epsilon))e^{-h\epsilon}, \quad h \in \mathbb{N} \quad (42)$$

Similarly, for BD neighbourhood case and $\delta = 0$ in Lemma 4 as $n \rightarrow \infty \implies b \rightarrow \infty$, from (26) we get:

$$\phi_0 \equiv 1 - \rho^*(\epsilon) \rightarrow \left(1 + \frac{\bar{\mu}e^{-\epsilon}}{1 - e^{-\epsilon}} \right)^{-1} \quad (43)$$

$$\implies \rho^*(\epsilon) \rightarrow \frac{\bar{\mu}e^{-\epsilon}}{\bar{\mu}e^{-\epsilon} + (1 - e^{-\epsilon})} \quad (44)$$

So, the expression for $\rho^*(\epsilon)$ for any $\epsilon > 0$ is:

$$\rho_\infty^*(\epsilon) = \begin{cases} 0.5, & \epsilon \in (0, \ln(1 + \bar{\mu})] \\ \frac{\bar{\mu}e^{-\epsilon}}{\bar{\mu}e^{-\epsilon} + (1 - e^{-\epsilon})}, & \epsilon \geq \ln(1 + \bar{\mu}). \end{cases} \quad (45)$$

Each of the PMF staircase steps becomes of size $\bar{\mu}$ and the values have an exponentially decaying trend:

$$f_\infty^*(0) = 1 - \rho_\infty^*(\epsilon) \quad (46)$$

$$f_\infty^*(\eta) = f_\infty^*(0)e^{-h\epsilon}, \quad (h-1)\bar{\mu} < \eta \leq h\bar{\mu}, \quad h \in \mathbb{N}^+. \quad (47)$$

For $0 < \delta \leq 1$, it is convenient to use the index $i = n - k$ looking at the trend of the distortion from $\delta = 1$, where $f^*(0) = 1$ backward. Because the discontinuities between flat and linear regions happen at the points where $\delta = \delta_{n-i}^\epsilon$, $i \in [n-1]$ we can see from Theorem 1 the distortion for $i \in [n-1]$:

$$f_i^*(0) \leq \frac{1-e^{-\epsilon}}{1-e^{-(i+1)\epsilon}} \Rightarrow \rho^*(\delta, \epsilon) \geq 1 - \frac{1-e^{-\epsilon}}{1-e^{-(i+1)\epsilon}}, \quad (48)$$

and the size of the intervals shrinks like an $o(e^{-i\epsilon})$, as $i \rightarrow +\infty$ quickly leading to the same result as $\delta \rightarrow 0$, where distortion tends to the same limit equal to $e^{-\epsilon}$ as stated before.

Similarly, for BD neighbourhood case, to find the expressions for ϕ_0^∞ and ϕ_i^∞ , it is convenient to use a new index $c = b - h$, looking at the trends of the distortion from $\delta = 1$, where $f^*(0) = 1$, going backwards towards $\delta = 0$. In the b^{th} segment (part (c) of Theorem 2, $f_b^*(\eta) \rightarrow 0$ as $b \rightarrow \infty$ and $n \rightarrow \infty$ for $\eta \in [n]_+$ and thus $f_b^*(0) \rightarrow 1$. For $\delta \approx 1$, in the c^{th} region we get the following expressions by using (31):

$$\alpha_{b-c,j}^\epsilon \rightarrow \frac{e^{-\epsilon}}{1-e^{-\epsilon}}; \quad \beta_{b-c,j}^\epsilon \rightarrow 1 - \frac{e^{-(c+j+1)\epsilon}}{1-e^{-\epsilon}} \quad (49)$$

$$\Rightarrow \phi_0^\infty(c, j) \rightarrow \frac{1-e^{-\epsilon}}{\mu e^{-\epsilon} + (1-e^{-\epsilon}(1+e^{-(c+j)\epsilon}))}, \quad (50)$$

$$\phi_i^\infty \rightarrow e^{-i\epsilon} \phi_0^\infty, \quad i \in [b+1]_+. \quad (51)$$

Now, as $c \rightarrow \infty$, the expression of $\phi_0^\infty(c, j)$ in (50) converges to ϕ_0 as shown in (43), i.e. the result for $\delta \rightarrow 0$.

4) *Optimal Noise Mechanism for Vector Queries:* Now, we briefly discuss the optimal noise mechanism design for vector queries. The MILP formulation of the problem defined in (11a)–(11f) can be applied directly to vectors of queries by simply considering the masses of probabilities as a joint PMF, with arguments corresponding to all possible tuples in \mathcal{Q}^k . In Section IV, we provide two examples for 2D vector queries—one for BD neighbourhood and another for arbitrary neighbourhood (see Fig. 11). We observe that for BD neighbourhood case, the optimum noise mechanism follows staircase pattern in 2D as well and for arbitrary neighbourhood, the optimum noise mechanism has $e^{-\epsilon} f^*(0)$ values at $\eta = \mu_{xx}$.

Remark 3. In general, the optimal multidimensional noise mechanism does not amount to adding independent random noise to each query entry, i.e., the marginal distribution of $f^*(\eta)$ is not equal to the optimum scalar PMF $f^*(\eta)$. In Section IV we corroborate this statement by showing a counter example obtained using the MILP program for the vector case, considering a two dimensional vector query.

IV. NUMERICAL RESULTS

In the literature, some contributions are made in providing the noise mechanisms for discrete queries such as geometric distribution [5], [15] or a quantized Gaussian distribution, as proposed in [11]. First, we find the (ϵ, δ) —differential privacy trade offs for the addition methodologies based on these mechanisms and compare them to highlight the effect of clamping. The clamping is an operation in which the query response \tilde{q} is projected onto the domain that is often used for the query $q \in [n]$ for any $\eta \in \mathbb{Z}$ [5], i.e.:

$$\tilde{q} = \min(\max(0, q + \eta), n). \quad (52)$$

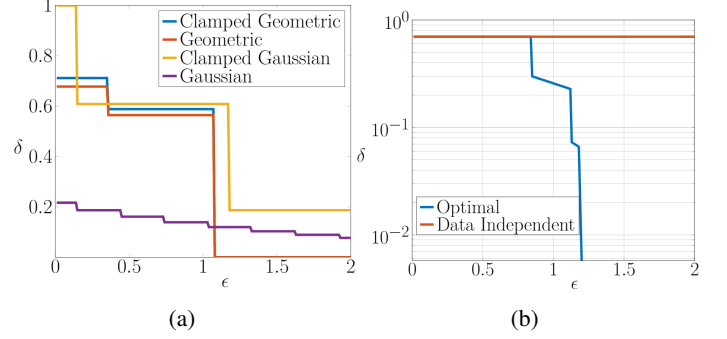


Fig. 5: Plot (a) shows the adverse effect of clamping operation on the (ϵ, δ) trade off for discrete geometric and discrete Gaussian mechanisms. The following parameters are used: $n = 8, \alpha = 0.7$ and $\sigma^2 = 3.38$. Plot (b) shows the comparison of the (ϵ, δ) trade off between the optimal noise mechanism with that of data independent noise mechanism, i.e. $f(0) = 1 - \rho$, $f(\eta) = \rho/n$, $\eta \in [n]_+$, for the same error rate $\rho = 0.3$.

Let $F_\eta(\eta)$ denote the cumulative distribution function of η ; then the distribution of \tilde{q} in terms of the distribution of η after clamping is as follows:

$$f_{\tilde{q}}(k|q) = \begin{cases} F_\eta(-q), & k = 0 \\ f_\eta(k - q), & k \in [n-1]_+ \\ 1 - F_\eta(n - q) & k = n. \end{cases} \quad (53)$$

From (53) one can compute the (ϵ, δ) privacy curve using (1), (2) and (53). After clamping the (ϵ, δ) guarantees provided by the said DP mechanisms are different from the ones calculated for $n = +\infty$ as shown in Fig. 5a, which are plotted for the same MSE = 3.38. From the figure it is clear that clamping increases δ for the same ϵ budget, and this effect is particularly pronounced in the case of the Gaussian mechanism. Hence, it is not advisable to use the infinite support based noise mechanisms, such as discrete geometric and discrete Gaussian, in tandem with clamping operations to publish the discrete query response with finite support.

Next, we compare the performance of our proposed optimal noise mechanism with state of the art discrete noise mechanisms proposed in the literature. In particular, we consider the discrete geometric mechanism [5], discrete Gaussian mechanism [11], and discrete count mechanism [10]. For the purpose of comparisons, we modify the MILP to the problem of minimizing δ with error rate ρ as a constraint (see Remark 1) and solve the MILP numerically using Gurobi solver. For a fair comparison, we consider the measure of errors, viz., error rate (ER) and mean square error (MSE), and respective parameters of the noise mechanisms viz., α in [5], σ^2 in [11], and ρ in [10], appropriately; the results are shown in Fig. 6.

In plot 6a, we show the comparison of the proposed optimal noise mechanism with the discrete geometric and discrete Gaussian mechanisms for a given MSE = 0.6101. Similarly, in plot 6b, we show the comparison of the proposed optimal noise mechanism with the discrete Gaussian mechanism and discrete count mechanisms for a given ER = 0.3. From the

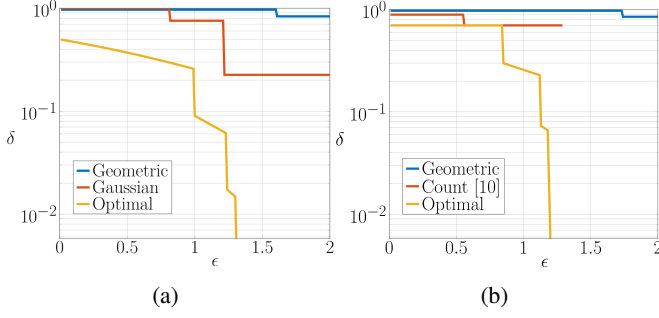


Fig. 6: Comparison of the proposed optimal mechanism in terms of (ϵ, δ) trade-offs with those proposed in [5], [10], [11]. In plot (a), the optimal noise mechanism is compared with the discrete geometric mechanism and discrete Gaussian mechanism for a fixed MSE, i.e., $\rho_{Geo.}^{MSE} = \rho_{Gau.}^{MSE} = \rho_{Opt.}^{MSE} = 0.6101$ and $n = 8$. In plot (b), the optimal noise mechanism is compared with the discrete geometric mechanism and discrete count mechanism for a fixed ER, i.e., $\rho_{Geo.}^{ER} = \rho_{Cnt.}^{ER} = \rho_{Opt.}^{ER} = 0.3$ and $n = 7$.

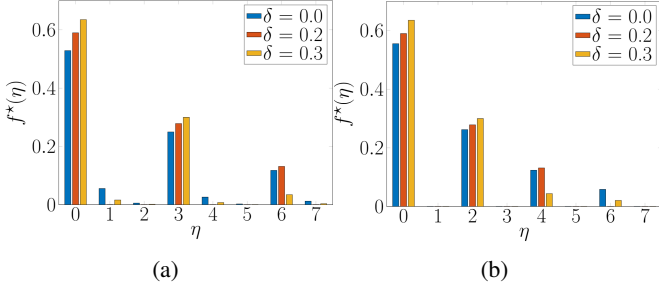


Fig. 7: These plots show the PMF of the optimal noise mechanisms for SD neighbourhood case and the following parameter values are used for both $n = 7, \epsilon = 0.75$. $\hat{\mu} = 3$ is used in plot (a), whereas $\hat{\mu} = 2$ in used in plot (b).

plots it is clear that the proposed optimal noise mechanism significantly outperforms all these mechanisms $\forall \epsilon > 0$.

In the following figures we show the structure of the PMF associated to the optimal noise mechanism. First, we consider single distance (SD) neighbourhood case. More specifically, the plots in Fig. 7 show the PMF of the optimal noise mechanisms, $f^*(\eta), \eta \in [n]$, for SD neighbourhood case for $\hat{\mu} = 3$ in Fig. 7a and for $\hat{\mu} = 2$ in Fig. 7b. In the left plot, we see that $f^*(\eta)$ is non-zero for all $\eta \in [n]$ since $(n+1, \hat{\mu})$ are relatively prime but in the right plot, we see that $f^*(\eta)$ is zero for $\eta \in \{1, 3, 5, 7\}$, since $(n+1, \hat{\mu})$ are not relatively prime (see Fig. 2 for the reasoning). From the plots we observe that as δ increases, $f^*(0)$ increases and since error rate, ρ^{ER} , is $1 - f^*(0)$ it decreases with increase in δ . And in the right plot, at some of the $\eta \in [n]_+$ values, zero probability mass is assigned. Hence, we see higher value of $f^*(0)$ compared to the corresponding values in the left plot, thus having the lower error rate in the right plot for a given δ value. Recall Lemma 2 and Lemma 3, to see that $f^*(0) \geq f^*(3) \geq f^*(6) \geq f^*(1) \geq f^*(4) \geq f^*(7) \geq f^*(2) \geq f^*(5)$ in Fig. 7a which are represented using $f^*(i), i \in [n]$, respectively.

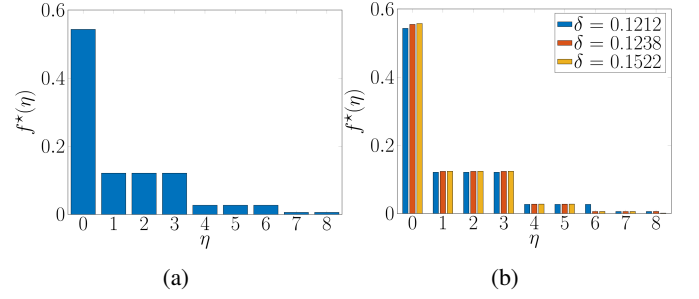


Fig. 8: These plots show the PMF of the optimal noise mechanisms for BD neighbourhood case and the following parameter values are used: $n = 8, \bar{\mu} = 3, \epsilon = 1.5$. In plot (a) we see that the optimal noise mechanism follows staircase pattern starting from $\eta = 1$ with $b = 2$ steps of length $\bar{\mu} = 3$ and one last step of length $r = 2$. In plot (b) we show how staircase pattern and step lengths change with δ . It can be seen at $\delta = \bar{\delta}_0^\epsilon = 0.1212$, $\delta = \bar{\delta}_1^\epsilon = 0.1238$, and $\delta = \bar{\delta}_2^\epsilon = 0.1522$ step lengths are: (1,3,3,2) (blue coloured bars), (1,3,2,3) (red coloured bars), and (1,3,2,2,1) (yellow coloured bars), respectively.

Similarly, we observe $f^*(0) \geq f^*(2) \geq f^*(4) \geq f^*(6)$ and rest $f^*(1) = f^*(3) = f^*(5) = f^*(7) = 0$ in Fig. 7b. Next, we consider the bounded difference (BD) neighbourhood case. The plots in Fig. 8 show the PMF of the optimal noise mechanisms, $f^*(\eta), \eta \in [n]$, for BD neighbourhood case for $\delta = 0$ in Fig. 8a and for $\delta > 0$ in Fig. 8b. In the left plot, we clearly see the staircase pattern with step sizes equal to $\bar{\mu}$, except for the last step. In the right plot, we see that step widths change as δ increases its values while the staircase structure is maintained. Note that vertical height of each step is e^ϵ times higher than the previous one, as can be seen in Fig. 8 and in Table I. Also, from the plot in Fig. 8b and Table I, one can observe as the value of $f^*(0)$ increases (thus the value of ρ^{ER} decreases) as δ increases, as it is expected. Next, we

	$\delta = 0$	$\delta = 0.1212$	$\delta = 0.1238$	$\delta = 0.1522$
$f^*(0)$	0.5432	0.5432	0.5548	0.5575
$f^*(1)$	0.1212	0.1212	0.1238	0.1244
$f^*(2)$	0.1212	0.1212	0.1238	0.1244
$f^*(3)$	0.1212	0.1212	0.1238	0.1244
$f^*(4)$	0.0270	0.0270	0.0276	0.0278
$f^*(5)$	0.0270	0.0270	0.0276	0.0278
$f^*(6)$	0.0270	0.0270	0.0062	0.0062
$f^*(7)$	0.0060	0.0060	0.0062	0.0062
$f^*(8)$	0.0060	0.0060	0.0062	0.0014

TABLE I: The PMF of the optimal noise mechanism for different values of δ for $n = 8, \bar{\mu} = 3, \epsilon = 1.5$.

consider the vector query case, and provide a counter example to support Remark 3 for a two dimensional vector query. Let $n = 4, \epsilon_1 = 1.5, \epsilon_2 = 1.5, \epsilon = 3, \mu_{XX'} = \{0, 1, 2\}, \delta = 0$. The optimal noise mechanism for $(\epsilon_1, 0)$ and $(\epsilon_2, 0)$ DP are: $f_1^*(\eta) = f_2^*(\eta) = [0.6469, 0.1443, 0.1443, 0.0322, 0.0322]$; the values of the optimal noise mechanism PMF $f^*(\eta_1, \eta_2)$ for $(\epsilon, 0)$ are in (54):

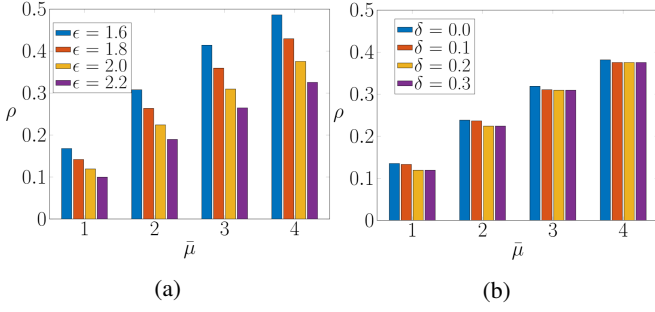


Fig. 9: These plots show the error rate for the BD neighbourhood case v/s parameter $\bar{\mu}$. In plot (a) $n = 9$, $\delta = 0.2$, and in plot (b) $n = 9$, $\epsilon = 2$ are used.

$$\begin{bmatrix} 0.6954 & 0.0346 & 0.0346 & 0.0017 & 0.0017 \\ 0.0346 & 0.0346 & 0.0346 & 0.0017 & 0.0017 \\ 0.0346 & 0.0346 & 0.0346 & 0.0017 & 0.0017 \\ 0.0017 & 0.0017 & 0.0017 & 0.0017 & 0.0017 \\ 0.0017 & 0.0017 & 0.0017 & 0.0017 & 0.0017 \end{bmatrix} \quad (54)$$

The marginal distributions happen to be equal, which makes sense in terms of symmetry: $f_1(\eta_1) = \sum_{\eta_2=0}^n f^*(\eta_1, \eta_2) \equiv f_2(\eta_2)$ and they have masses $[0.7681, 0.1073, 0.1073, 0.0086, 0.0086]$. We can observe that $f^*(\eta_1, \eta_2) \neq f_1(\eta_1)f_2(\eta_2)$.

The plots in Figs. 9–12 are self explanatory.

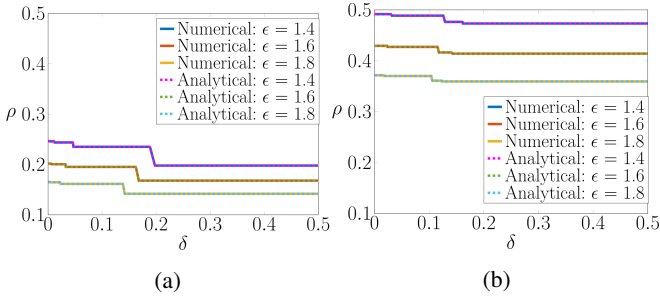


Fig. 10: Error rate ρ for the SD and BD neighbourhood cases v/s parameter δ , respectively, confirming the trends predicted by Theorems 1 and 2. In plot (a) $n = 9$, $\bar{\mu} = 3$ and in plot (b) $n = 9$, $\bar{\mu} = 3$ are used.

V. CONCLUSIONS AND FUTURE WORK

Considering queries whose domain is discrete and finite, in this paper we proposed a novel MILP formulation to determine what is the PMF for an additive noise mechanism that minimizes the error rate of the DP answer for any (ϵ, δ) pair. The modulo addition between the noise and the queried data are modulo $n + 1$ equal to the size of the query domain. For two special cases, which we referred to as the single distance (SD) neighbourhood and bounded difference (BD) neighbourhood, we have provided closed form solutions for the optimal noise PMF and its probability of error versus δ for a given ϵ and studied the asymptotic case for $n \rightarrow \infty$. We also compared the proposed optimal noise mechanism to state-of-the-art noise mechanisms and found that it significantly

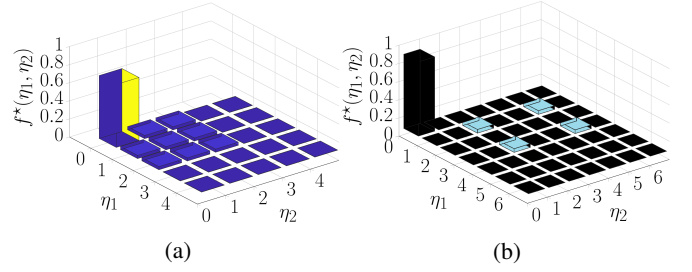


Fig. 11: The optimal noise joint PMF for two dimensional vector query case for a BD and an arbitrary neighbourhoods, respectively. In plot (a) the parameters are: $n = 4$, $\epsilon = 3$, $\bar{\mu}_1 = \bar{\mu}_2 = 2$. In this BD neighbourhood example the staircase pattern is similar to scalar query case in Theorem 2. In plot (b) the following parameters are used: $n = 6$, $\epsilon = 3$, $\mu_1 = \{1, 3\}$, $\mu_2 = \{2, 5\}$. In this arbitrary neighbourhood example, the second largest peaks can be observed at the union of distance one sets of each dimension, i.e., $[1, 2]$, $[1, 5]$, $[3, 2]$, $[3, 5]$.

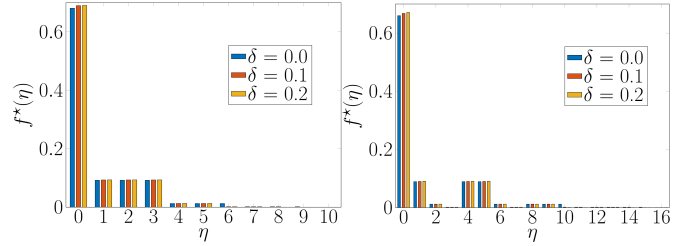


Fig. 12: These plots show the PMF of the optimal noise mechanisms when the Advanced Metering Infrastructure (AMI) database is queried for quantized power consumption of 25 houses for a given day. We use $\bar{\mu} = \bigcup_{X \in \mathcal{X}} \bigcup_{X' \in \mathcal{X}_X^{(1)}} \mu_{X'}$. In the left plot, 11 quantization levels are used, hence $n = 10$. In this example, $\bar{\mu} = \{1, 2, 3\}$ is observed. In the right plot, 17 quantization levels are used, hence $n = 16$. In this example, $\bar{\mu} = \{1, 4, 5\}$ is observed.

outperforms them for a given error rate. In the future we plan to leverage these results in several applications that have to do with labeling data as well as a building block to study theoretically queries with finite uncountable support as well as the case of vector queries, whose optimum PMF can be calculated with our MILP and does not appear to be the product of the optimum PMFs for each entry.

REFERENCES

- [1] US Bureau of the Census, Disclosure Avoidance and the 2020 Census, URL: <https://www.census.gov/programs-surveys/decennial-census/decade/2020/planning-management/process/disclosure-avoidance.html>
- [2] A. Eland, Tackling Urban Mobility with Technology. Google Policy Europe Blog, Nov 18, 2015. <https://europe.googleblog.com/2015/11/tackling-urban-mobility-with-technology.html>
- [3] B Ding, J Kulkarni, S Yekhanin, Collecting Telemetry Data Privately, Proc. of International Conference on Neural Information Processing Systems, pp. 3574–3583 (2017).
- [4] R. Rogers, et al., LinkedIn’s Audience Engagements API: A Privacy Preserving Data Analytics System at Scale, [arXiv:2002.05839](https://arxiv.org/abs/2002.05839)v3 (2020).

- [5] A. Ghosh, T. Roughgarden, M. Sundararajan, Universally Utility-Maximizing Privacy Mechanisms. *SIAM J. Comput.* 41, pp. 1673–1693 (2012), DOI: 10.1145/1536414.1536464.
- [6] J. Soria-Comas, J. Domingo-Ferrer, Optimal Data-Independent Noise for Differential Privacy, *Inf. Sci.*, vol. 250, pp. 200–214 (2013), DOI:10.1016/j.ins.2013.07.004.
- [7] Q. Geng, P. Viswanath, Optimal Noise Adding Mechanisms for Approximate Differential Privacy, *IEEE Trans. Inf. Theory*, vol. 62, no. 2, pp. 952–969 (2016), DOI: 10.1109/TIT.2015.2504972.
- [8] Q. Geng, P. Viswanath, The Optimal Noise-Adding Mechanism in Differential Privacy, *IEEE Trans. Inf. Theory*, vol. 62, no. 2, pp. 925–951 (2016), DOI: 10.1109/TIT.2015.2504967.
- [9] G. Cormode, T. Kulkarni, D. Srivastava, Constrained Private Mechanisms for Count Data, *IEEE Trans. Knowl. Data Eng.*, vol. 33, no. 2, pp. 415–430 (2021), DOI: 10.1109/TKDE.2019.2912179.
- [10] P. Sadeghi, S. Asodeh, F.P. Calmon, Differentially Private Mechanisms for Count Queries, *arXiv:2007.09374v1* (2020).
- [11] C. Canonne, G. Kamath, T. Steinke, The Discrete Gaussian for Differential Privacy, *arXiv:2004.00010v5* (2020).
- [12] Q. Geng, P. Kairouz, S. Oh, P. Viswanath, The Staircase Mechanism in Differential Privacy, *IEEE J. Sel. Top. Signal. Process.*, vol. 9, no. 7, pp. 1176–1184 (2015), DOI: 10.1109/JSTSP.2015.2425831.
- [13] A. Triastcyn, B. Faltings, Bayesian Differential Privacy for Machine Learning, *Proc. of International Conference on Machine Learning*, pp. 9583–9592 (2020).
- [14] Gurobi Optimization Solver, <https://www.gurobi.com/>
- [15] V. Balcer, S. Vadhan, Differential Privacy on Finite Computers, *J. priv. confid.*, vol. 9, no. 2 (2019), DOI: 10.29012/jpc.679.

APPENDIX

A. Proof of Lemma 2

From the inequality constraint in (11b), we see that $f_{(0)}^* = f^*(0) \geq 0.5$, since $\sum_{k=0}^n f^*(k) = 1$ (see (12b)). Hence, $f_{(0)}^* = \sup_{\eta \in [n]} f^*(\eta)$. Now, substitute $\eta = 0$ and $\mu_{xx} = \hat{\mu}$ in (12c) we see that $f^*(0) \leq e^\epsilon f^*(\hat{\mu})$. Since we are minimizing the sum of the mass away from zero, we assign $f^*(\hat{\mu})$ to the minimum possible value, which is $f^*(\hat{\mu}) = e^{-\epsilon} f^*(0)$ in this case. Similarly, from (12c) we see that $f^*(k\hat{\mu}) \leq e^\epsilon f^*((k+1)\hat{\mu})$, $k \in [n-1]_+$, and we are minimizing the sum of the mass away from zero, we need to assign $f^*((k+1)\hat{\mu})$ to the minimum possible value, which is $f^*((k+1)\hat{\mu}) = e^{-\epsilon} f^*(k\hat{\mu})$.⁴ Since $\epsilon > 0$, $f^*(k\hat{\mu}) \geq f^*((k+1)\hat{\mu})$, $\forall k \in [n]$. Hence, we can write $f_{(k)}^* = f^*(k\hat{\mu})$, $\forall k \in [n]$.

B. Proof of Lemma 3

Case 1: $(\hat{\mu}, (n+1))$ are relatively prime.

The proof logic is as follows. Since minimizing the error rate is equivalent to have the maximum mass possible at $\eta = 0$, we expect $f^*(0) = \sup_{\eta \in [n]} f^*(\eta)$. The constraint (13), implies $f^*(\hat{\mu}) \geq e^{-\epsilon} f^*(0)$. Also that for any $\eta = k\hat{\mu}$, $k \in [2 : n]$, $f^*(k\hat{\mu}) \geq e^{-\epsilon} f^*((k-1)\hat{\mu}) \geq e^{-k\epsilon} f^*(0)$ and $f^*((n+1)\hat{\mu}) = 0 \geq e^{-\epsilon} f^*(n\hat{\mu})$. From all these inequalities and the constraint (12a), we conclude that what would allow to have the largest mass of probability at $\eta = 0$ is meeting all constraints as an equality, starting from the first. Since $\hat{\mu}$ and n are prime, the multiples of $\hat{\mu}$ eventually cover the entire range $[n]$ and therefore: $f^*(k\hat{\mu}) = e^{-k\epsilon} f^*(0)$, $k \in [n]$. This

⁴Note that for $f^*(n\hat{\mu})$, there is no choice to assign any value since it will be automatically fixed once $f^*(k\hat{\mu})$, $k \in [n-1]$ values are fixed and it is trivial to see that $f^*(n\hat{\mu}) = \min f^*(k\hat{\mu})$, $\forall k \in [n]$.

result leads to the optimum distribution in Lemma 3. Now, $f^*(0)$ can be computed as follows:

$$f^*(0) + e^{-\epsilon} f^*(0) + \dots + e^{-n\epsilon} f^*(0) = 1 \quad (55a)$$

$$f^*(0) = \frac{1 - e^{-\epsilon}}{1 - e^{-(n+1)\epsilon}}. \quad (55b)$$

Case 2: $(\hat{\mu}, (n+1))$ are not relatively prime.

The same argument of Case 1 holds for $k \in [N_{\hat{\mu}} - 1]_+$, where $N_{\hat{\mu}} = \frac{(n+1)}{\gcd((n+1), \hat{\mu})}$, i.e., $f^*(k\hat{\mu}) = e^{-k\epsilon} f^*(0)$, $k \in [N_{\hat{\mu}} - 1]_+$. However in this case, since for $k = N_{\hat{\mu}}$, $f^*(N_{\hat{\mu}}\hat{\mu}) = f^*(0)$ and the cycle repeats over the same exact values covered from zero up to $(N_{\hat{\mu}} - 1)$ which does not include all PMF entries. Since we are minimizing the objective function to satisfy all the inequality constraints in (11b) and (13) for all k values that are not constraining $f^*(0)$, the best choice is to assign them zero, i.e., $f^*(k) = 0$, $k \in [n] \setminus [i\hat{\mu}]$, $\forall i \in [N_{\hat{\mu}} - 1]$.

C. Proof of Theorem 1

We focus on Case 1, as Case 2 is similar as specified in Remark 2. In Lemma 2 we clarified that is best to deal with the ordered values and, in Lemma 3, we specified $f_{(h)}^*$, $h \in [n]$, as a function of $\epsilon > 0$ for $\delta = 0$. The best solution for $\rho(\epsilon, \delta)$ initially does not change until violating an inequality in (13) yields better accuracy. This happens as soon as the second smallest value $f_{(n-1)}^*$ corresponding to $\delta = 0$ is $f_{(n-1)}^* = \delta$, which is the upper-limit $\bar{\delta}_0$ from (16). The reason why it is $f_{(n-1)}^*$ and not $f_{(n)}^*$ that matters, is because surely $f_{(n)}^* < e^\epsilon f_{(0)}^*$ which in the modulo n sum is the value that follows and that we aim at maximizing. At this point, for $\bar{\delta}_0 < \delta \leq \underline{\delta}_1$ the value of $f_{(n-1)}^* = \delta$, all the values for $0 \leq h < n-1$ meet the constraints with equality and thus $f_{(h)}^* = e^{(n-1-h)\epsilon} \delta$, while the last value $f_{(n)}^*$ progressively diminishes until it becomes zero, as shown in equation (18), at the start of the next flat region. This pattern continues until eventually one by one all $n-1$ masses become zero except for $f^*(0) = 1 = \underline{\delta}_n^\epsilon$.

D. Proof of Theorem 2

In Lemma 4, we have the expressions for ϕ_i , $i \in [b+1]_+$ for $\epsilon > 0$ and $\delta = 0$. The best solution for $\rho^*(\delta, \epsilon)$ does not change w.r.t $\delta > 0$ until violating an inequality in (24) to yield better accuracy. The key to the proof is understanding that the first inequality to be violated occurs when considering δ greater or equal not to the smallest PMF value but to the PMF values of the third to the last group in $\delta = 0$ case, i.e., $\phi_{b-1} = \delta$, whose value equals the first boundary point $\bar{\delta}_{0,0}^\epsilon$ (see (34a)). The inequality violated is with respect to the PMF of the second to the last group, which is ϕ_b , which becomes $= \delta$ and $\phi_{b-1} > e^\epsilon \delta$. The reason why the PMF of the last group, i.e. ϕ_{b+1} , does not violate the inequality in (24) is because $\phi_{b+1} < e^\epsilon \phi_0$ (we use ϕ_0 since we are doing modulo summation) is always true for all members of this group, due to the fact that ϕ_0 is the objective function which we are maximizing. Similarly, the PMF of the second last group, i.e. ϕ_b , does not violate the inequality in (24) because some members of this group do not violate the inequality $\phi_b < e^\epsilon \phi_0$ for the same reason as

stated above. At this point, for $\bar{\delta}_{0,0} < \delta \leq \bar{\delta}_{1,1}$ the value of $\phi_{b-1} = \delta$, the PMF values for $i \in [b-1]$ meet the constraints with equality and thus $\psi_i^1(\delta) = \delta e^{(b-1-i)\epsilon}$, for $i \in [b-1]$. At this point, the group with PMF ϕ_b , whose length is $\ell_b = \bar{\mu}$, splits into two groups, one of length $\ell_b = (\bar{\mu} - 1)$ and the other with a singleton step $\ell_{b+1} = 1$. This split happens to assign more probability mass at $\psi_0^1(\delta)$, which is our objective, while still violating the constraint in (24) between $\delta = \psi_{b-1}^1(\delta)$ and $\psi_{b+1}^1(\delta)$ in order to lower the error further. For $i = b$ and $i = b + 2$, the PMF values satisfy the constraints with equality, hence $\psi_b^1(\delta) = \delta e^{-b\epsilon}$ and $\psi_{b+2}^1(\delta) = \delta e^{-(b+1)\epsilon}$ while the unconstrained singleton step PMF $\psi_{b+1}^1(\delta)$ decreases until it joins the next group since it has matched its value, and becomes ϕ_{b+1}^1 , as shown in equation (27), at the start of the next flat region, i.e., for $\bar{\delta}_{1,1} \leq \delta \leq \bar{\delta}_{1,1}$. In this region, the PMF of every group is $e^{-\epsilon}$ times the PMF of previous group similar to Lemma 4; the only change here is the lengths of b^{th} and $(b+1)^{th}$ groups which are now $\ell_b = (\bar{\mu} - 1)$ and $\ell_{b+1} = r + 1$.

Now we provide the reason for splitting of only groups of lengths $\bar{\mu}$ using contradiction. Suppose there is a group i of length $\ell < \bar{\mu}$ which splits at the beginning of a linear region $k \in [b]_+$. As we know, for this group to split there must a violation of the inequality in (24) between the PMF values $\phi_{i-1}^{k-1} = \delta$ and ϕ_i^{k-1} . Now, ϕ_i^{k-1} splits into $\psi_i^k(\delta)$ of length $(\ell - 1)$ and $\psi_{i+1}^k(\delta)$ of length 1, which decreases as δ grows. We see that $\psi_{i+1}^k(\delta)$ is $\leq \bar{\mu}$ distance away from at least two members of the $\psi_{i-1}^k(\delta)$ group leading to at least two violations in the inequalities in (24) which makes the actual privacy loss $\geq 2\delta$, in violation of the inequality constraint in (11c), which is a contradiction.

From the discussion in the previous paragraph, for the next linear region we now search for a group of length $\bar{\mu}$ with smallest possible PMF, which is found to be $(b-1)^{th}$ group, whose PMF is ϕ_{b-1}^1 . For this group to split and enter into the linear region, we should have $\delta = \phi_{b-2}^1$. As explained in the first paragraph of this proof, the same process follows in this linear region too, i.e., for $\bar{\delta}_{1,1} < \delta \leq \bar{\delta}_{2,1}$. In the next flat region, i.e., for $\bar{\delta}_{2,1} \leq \delta \leq \bar{\delta}_{2,1}$ the step lengths, as compared to previous flat region, which have been altered are $\ell_{b-1} = (\bar{\mu} - 1)$ and $\ell_b = \bar{\mu}$. Now, observe that b^{th} group has length $\bar{\mu}$ and from the discussion in the previous paragraph, this group splits at the end of this flat region, i.e., when $\delta = \phi_{b-2}^2 + \phi_{b-1}^2 = \phi_0^2 e^{-(b-2)\epsilon} (1 + e^{-\epsilon}) \equiv \bar{\delta}_{2,1}$. In this case the inequality in (24) are violated by both ϕ_{b-2}^2 and ϕ_{b-1}^2 , hence the summation and the reasoning for (34a) (this was missing in SD neighbourhood case). For the same reason, in the next linear region i.e., for $\bar{\delta}_{2,1} < \delta \leq \bar{\delta}_{2,2}$ the normalizing factor $(1 + e^{-\epsilon}) \equiv \xi_2^\epsilon$ is used while computing the PMF values in (36).

These alternate flat and linear intervals are formed as δ increases and the process continues until all the remaining groups of lengths $\bar{\mu}$ split into groups of lengths $(\bar{\mu} - 1)$. The expression for $\underline{\delta}_{h,j}$, $h \in [b-1]_+$, $j \in [h]_+$ in (34b) is computed using $f^*(0)$ vs. δ curve (see Fig. 4) in the linear region between ϕ_0^{k-1} and ϕ_0^k , the slope corresponding to $\psi_0^k(\delta)$

i.e. $e^{(b-h)\epsilon}/\xi_j^\epsilon$ from (36). i.e.,

$$\begin{aligned} \underline{\delta}_{h,j} &= \bar{\delta}_{h,j-1}^\epsilon + (\phi_0^k - \phi_0^{k-1})e^{-(b-h)\epsilon}\xi_j^\epsilon \\ &= \phi_0^{k-1}e^{-(b-h)\epsilon}\xi_j^\epsilon + (\phi_0^k - \phi_0^{k-1})e^{-(b-h)\epsilon}\xi_j^\epsilon \\ &= \phi_0^k e^{-(b-h)\epsilon}\xi_j^\epsilon. \end{aligned} \quad (56)$$

Now, we find the simplified expression for the value of ϕ_0^k from the fact that $\phi_0^k + \sum_{i=1}^{b+1} \ell_i \phi_i^k = 1$ as following:

$$\begin{aligned} \phi_0^k &\left(1 + \bar{\mu} \sum_{i=1}^{b-h} e^{-i\epsilon} + (\bar{\mu} - 1) \sum_{\substack{i=b-h+1 \\ i \neq b-h+j+1}}^b e^{-i\epsilon} \right. \\ &\quad \left. + \bar{\mu} u_{hj} e^{-(b-h+j+1)\epsilon} + (r+h-u_{hj})e^{-(b+1)\epsilon} \right) = 1 \end{aligned} \quad (57)$$

By further simplifying, we get:

$$\begin{aligned} \phi_0^k &= \left(1 + \bar{\mu} \sum_{i=1}^b e^{-i\epsilon} - \bar{\mu}(1 - u_{hj})e^{-(b-h+j+1)\epsilon} \right. \\ &\quad \left. + e^{-(b-h+j+1)\epsilon} + (r+h-u_{hj})e^{-(b+1)\epsilon} - \sum_{i=b-h+1}^b e^{-i\epsilon} \right)^{-1} \\ \phi_0^k &= (\bar{\mu}\alpha_{hj}^\epsilon + \beta_{hj}^\epsilon)^{-1}, \text{ see (31).} \end{aligned}$$

The last group has length $b + r$ which is less than $\bar{\mu}$ in our case. This assumption simplifies the analysis, hence tractable. Even though the pattern is same, the case $b + r \geq \bar{\mu}$ complicates the analysis because, for $j \in [h]_+$ and for every $h \in [b]_+$, instead of increasing h when $j = h$, j must be increased beyond h to accommodate the groups of lengths $\bar{\mu}$ created by the last group whenever its length $r + h$ exceeds $\bar{\mu}$. Hence, we do not discuss the analysis of this case, but we do provide some numerical results in Section IV.